

The Wheel-Individually Steerable Front Axle of the Research Vehicle SpeedE

Dipl.-Ing. Lars **Hesse**

fka mbH, Aachen, Germany

Benjamin **Schwarz** M.Sc., Dipl.-Ing. Michael **Klein**,

Univ.-Prof. Dr.-Ing. Lutz **Eckstein**

Institute for Automotive Engineering, RWTH Aachen University, Germany

Summary

The Institute for Automotive Engineering at RWTH Aachen University (ika), is currently developing, constructing, and implementing the research vehicle SpeedE as an open research and innovation platform for research and industry. The research focus of the SpeedE concept, amongst other things, is the innovative front suspension. Not only is the front axle's steer-by-wire system able to steer each wheel individually, but it is also able to achieve steering angles of up to 90°. The central core of the steering system is made up of two electric motors in combination with harmonic drive reduction gears integrated in the upper control arms of a double wishbone suspension, which is accompanied by a replacement of the outer ball joints of the upper control arm by cardan joints and an elimination of the tie rods. The focus of this article is to present the topology of the front axle and the development methodology used during the design of the front axle. Based on example challenges that had to be overcome by the requirements inherent in the system, the associated solutions implemented for the selection of the position of the steering axle, and the chassis attachment points as well as the orientation of the cardan joint are discussed in this paper.

1 Introducing the Research Vehicle SpeedE

The Institute for Automotive Engineering at RWTH Aachen University (ika), is currently developing, constructing, and implementing the research vehicle SpeedE as an open research and innovation platform for research and industry. The goal of the concept vehicle is to create a distinct added value to an electric vehicle, leading from electromobility to E-Motion [1]. The vehicle concept was developed in conjunction with the renowned Department of Transportation Design at Hochschule Pforzheim University, with the intent of combining design and technology in a new approach at an earlier stage of development.

After Nissan announced the introduction of steer-by-wire technology on selected Infiniti vehicles in 2012 [2], the SpeedE vehicle concept takes this concept a step further with a steer-by-wire system embedded in a concept of functional safety [3]. The research focus of the SpeedE concept, amongst other things, is the innovative

front suspension. This is because the front axle's steer-by-wire system is not only able to steer each wheel individually, but is also able to achieve steering angles of up to 90° . The central core of the steering system is made up of two electric motors in combination with harmonic drive reduction gears integrated in the upper control arms of a double wishbone suspension, which is accompanied by a replacement of the outer ball joints of the upper control arm by cardan joints and an elimination of the tie rods. In combination with electric rear axle torque vectoring, using the twin motors mounted on the rear axle, new maneuvering possibilities can be achieved through a turning circle with the rear, inside wheel set as the center of rotation. The advantages of this steering concept are emphasized by a driver control system with active side-sticks for enabling new driver's seat and entire interior design possibilities [4].

The focus of this article is to present the topology of the front axle and the development approach used during the design of the front axle. Based on example challenges that had to be overcome by the requirements inherent in the system, the associated solutions implemented for the selection of the position of the steering axle, and the chassis attachment points as well as the orientation of the cardan joint are discussed in this paper.

2 Topology of the Front Axle

Because of the individual wheel steering, it is possible to adjust the wheel steering angle independently and on an as needed basis. A steering angle of up to 90° can be achieved and thus a very high maneuverability of the vehicle as well. Also, the individual wheel steering angle causes an increase of the driving safety as well as the full utilization of the lateral force potential of the front axle. The maximum wheel steering angle in a parking situation is depicted in Fig. 1.

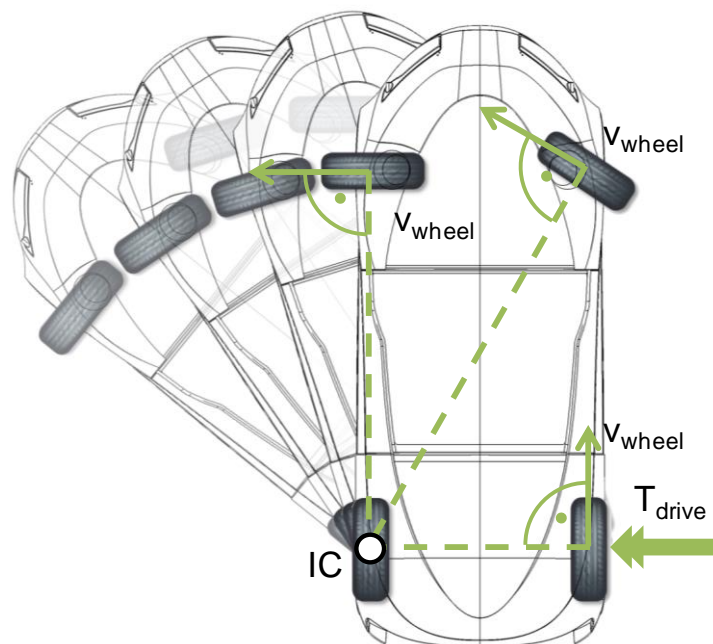


Fig. 1: Maximum Steering Angle while Parking

In the depicted sketch the left wheel is turned in by 90° and the right wheel by 60° . The wheel's velocity vectors correspond with the wheel planes, since, due to the low speed while parking, no significant side slip angles develop. This means that the instantaneous center of rotation (IC) of the vehicle movement is located at the rear inside wheel. The drive type of the vehicle consists of two wheel hub electric motors on the rear axle, so that a variable distribution of drive torque to the rear wheels is enabled. For the parking situation depicted in Fig. 1, only the outside rear wheel is driven, such that the vehicle turns around the inside rear wheel. The front portion of the vehicle has a rounded shape so that when turning around the rear wheel, no additional space is required at the front. The turn is feasible in both directions, so that the left front wheel can be turned in a range of -60 to 90° and the left front wheel can turn in the range of -90 to 60° .

In order to achieve these ranges of wheel steering angles, a double-wishbone suspension concept is chosen and modified according to the requirements. Without significant structural actions, conventional tie rods are not feasible with the large steering angles required. For this reason, two steering actuators which are mounted between the upper control arms and the wheel carriers substitute the conventional tie rods and also the rack and pinion steering gear. The axis of rotation of the individual wheel steering actuators is aligned with the steering axle of the suspension. An overview of the adapted double wishbone suspension concept for the front axle of the SpeedE research vehicle is shown in Fig. 2.

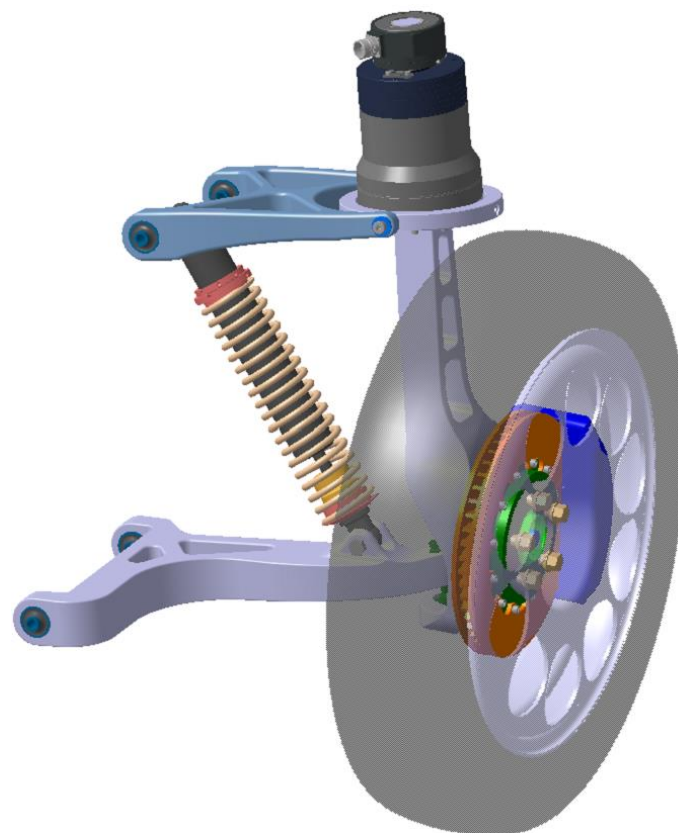


Fig. 2: Independent Suspension of the Front Axle of the SpeedE Research Vehicle

An electric motor combined with a reduction gear is implemented as the steering actuator. An important requirement of the reduction gear is a high rotational stiffness and highest possible freedom of play. In this concept, this is accomplished by a harmonic drive gear with a high transmission ratio. This configuration fully meets the requirements and allows a compact actuator unit with acceptable additional unsprung mass.

The articulated connection between the upper control arm and the wheel hub cannot be carried out by implementing a ball joint in this case, as is customary in the conventional double wishbone suspension concept. With this concept, a cardan joint connects the upper control arm with the wheel hub. Fig. 3 depicts the connection between the upper control arm and the wheel hub as well as the steering actuator.

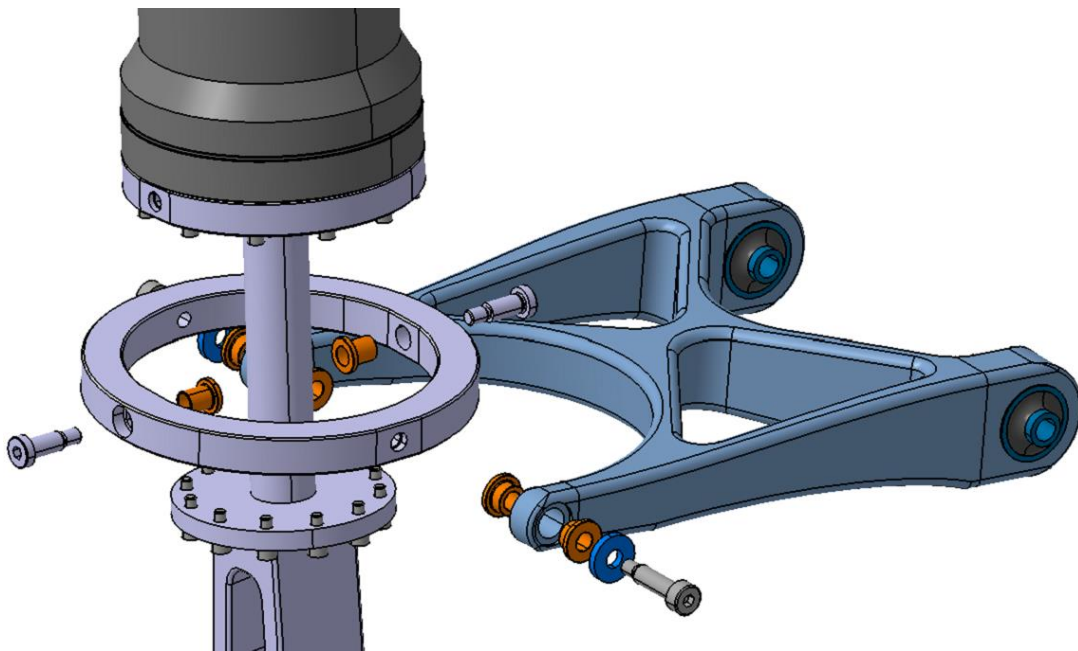


Fig. 3: Cardanic Connection between the Upper Control Arm and the Wheel Hub with Integrated Steering Actuator

Compared to a ball joint, the cardan joint locks an additional rotational degree of freedom, so the suspension has only the required degree of freedom to enable jounce and rebound motion of the wheel despite the absence of the tie rod. The position of the cardan joint is determined by the orientation of the outer and inner cardan ring and the according axis of rotation. The outer cardan ring is connected by means of two sliding bearings articulated with the upper control arm, so that a defined axis of rotation results. The steering actuator is bolted onto the inner cardan ring which is connected to the outer ring by two sliding bearings as well. The rotor's axis is oriented along the steering axis, which is defined by the outer kinematic points of the upper and lower control arms. Thus, the position of the inner cardan ring is dependent on both the orientation of the steering axle and the position of the outer cardan ring. The position of the outer cardan ring's axis of rotation relative to the position of the steering axle is critical for the toe angle change during wheel travel. The change in the relative position between the steering axle and the outer cardan

ring's axis of rotation during jounce movement is decisively influenced by the configuration of the outer cardan ring's axis of rotation to the upper control arm's axis of rotation. For this reason, the position of the cardan joint in the space, regarding the other axes of rotation of the suspension is important in the design of the kinematics.

To describe the orientation of the joints, the four angles α , β , ε , and γ are subsequently used. The center point of the cardan joint is determined by the outer kinematic point of the upper control arm.

For the design, only the angles α and β can be influenced as parameters. These angles describe the position of the outer cardan ring. The angles ε and γ are dependent on the position of the steering axis and the position of the outer ring, so that they are not independently adjustable design parameters. In Fig. 4 the orientation of the outer cardan ring is depicted as a function of the angles α and β .

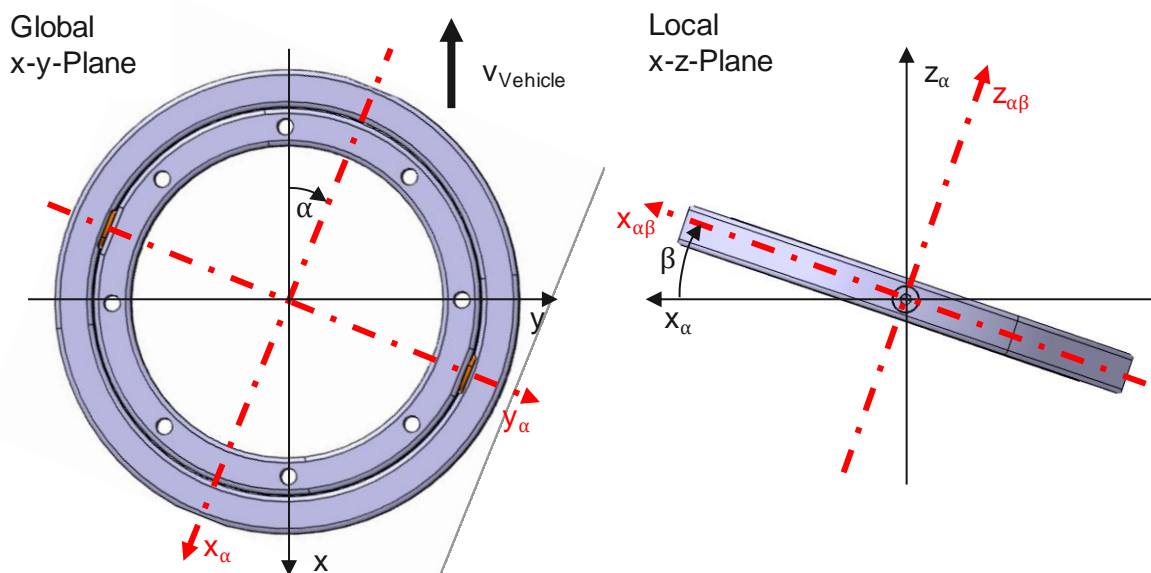


Fig. 4: Orientation of the outer Cardan Ring's Axis of Rotation

In the first step, the entire joint is rotated about the negative global z-axis by the magnitude of the angle α . Then, a rotation occurs about the negative y_{α} -axis of the body-fixed coordinate system, which differs from the rotation of the first step from the global coordinate system. This rotation is described by the angle β . Thus, the outer cardan joint's axis of rotation is now explicitly defined by the two angles and the outer point of the upper control arm. The position of the inner cardan joint results from the position of the steering axis and the outer cardan ring's axis of rotation. In Fig. 5 the position of the inner cardan ring is illustrated, which is described by the angles ε and γ .

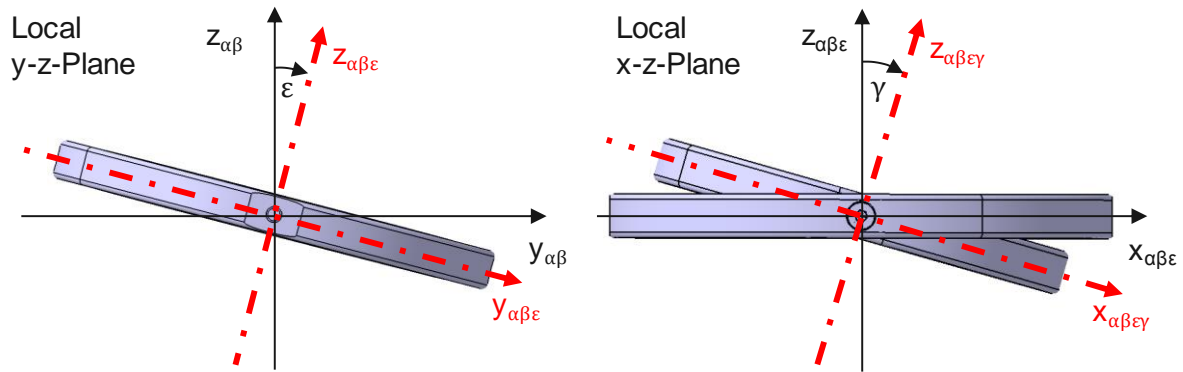


Fig. 5: Orientation of the inner Cardan Ring's Axis of Rotation

Based on the position of the outer cardan ring's axis of rotation, the axis of rotation of the inner ring is rotated about the body-fixed negative $x_{\alpha\beta}$ -axis with the angle ϵ . Therefore, the position of the joint's second axis of rotation is fully determined. Lastly, the inner ring rotates about its own axis, the body-fixed, negative $y_{\alpha\beta\epsilon}$ -axis with the magnitude of the angle γ . Now the $z_{\alpha\beta\epsilon\gamma}$ -axis of the inner cardan ring is located on the steering axle.

3 Approach for the Front Axle Design

The requirements of the front suspension design of the SpeedE research vehicle and the problem-solving approach derived from this are explained in the following section.

3.1 Design Requirements of the Front Axle Suspension

The requirements of the front suspension design result from, on one hand, the innovative concept of the suspension and, on the other hand, from the requirements that are posed by a conventional suspension concept.

The size of the scrub radius and the caster trail must meet enhanced requirements due to the limited torque potential of the steering actuator. Besides the transmission ratio of the reduction gear the torque that the electric motor must produce under applied braking and lateral forces highly depends on the lever arms between the tire contact point and the steering axis. These lever arms are determined by the scrub radius and the caster trail. Depending on the estimated braking and lateral forces, a maximum value is calculated for the scrub radius and the caster trail of 45 mm. So that no turning-in effect of the wheel occurs due to a lateral force, the minimum caster must amount to 15 mm in the positive direction. Further crucial design criteria are the king pin angle and the caster angle of the steering axis due to the effect on the change of camber angle during steering. The tire properties require the maximum camber angle to be limited to 10° .

The caster offset, as a further design criterion of the steering axis, is important for the position of the wheel relative to the chassis at the maximum steering angle. At a

wheel steering angle of 90° the caster offset is crucial for the horizontal position of the wheel center in relation to the vehicle center plane. This fact is illustrated in Fig. 6 with a sketch. In the left side of the figure the caster offset is positive and on the right side it is negative. The distance between the body structure and the steering axis is the same in both views. For a wheel steering angle of 90° , the distance between the body structure and the wheel is larger with a positive caster offset than with a negative caster offset. It can be seen that if too high a negative caster offset exists, there is a collision between the wheel and the body structure. Therefore the caster offset is set up in a way, that a collision is avoided.

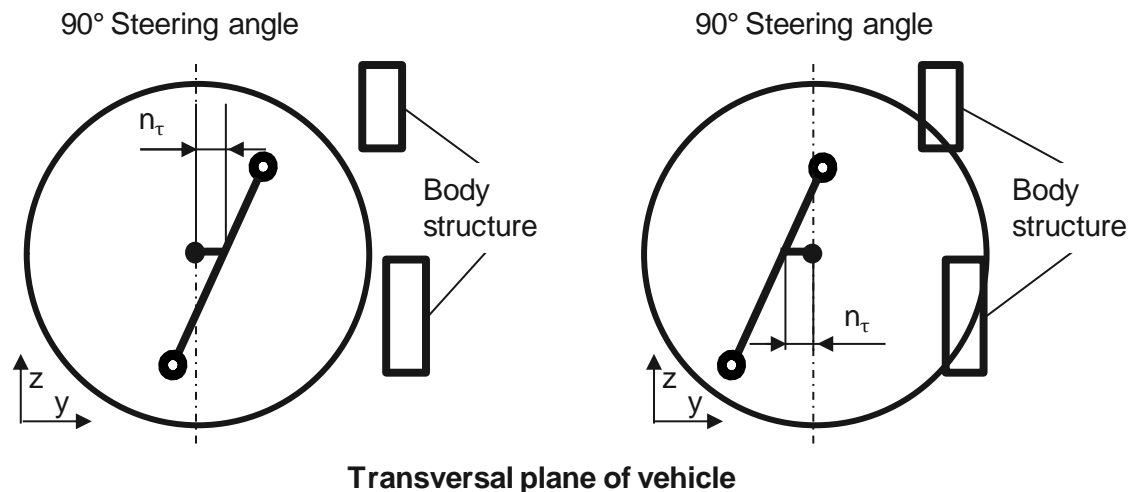


Fig. 6: Wheel Position for a Positive Castor Offset (Left) and a Negative Castor Offset (Right) with a Wheel Steering Angle of 90° in the Vehicle's Lateral Plane

The actual wheel steering angle is an important input parameter for the steering actuator controller. The installed sensor can only detect angles between the wheel carrier and the inner cardan ring, see Fig. 6. The sensor is not able to detect a change of toe angle due to lifting movement of the wheel. Therefore the toe angle has to experience a minimum amount of change during wheel travel. The envisioned goal is a maximum change of one angular minute for the entire lifting process

The additional requirements on the passive design of the front suspension are not derived from the innovative topology but instead could be taken from a conventional suspension design.

The largest possible contact area between the tires and the road surface is required to be able to transfer the maximum force in the contact patch. Without a change in camber of the tire during wheel travel, the tire contact patch is reduced by a body rolling movement. So the reduction of the tire contact patch as a result of a body rolling motion is compensated for, a progressive increase of negative camber is crucial while the suspension is in compression. For the roll center height change of

the front axle, it applies that a similar change is desirable during parallel wheel as it is present at the rear axle.

The target values for the elasto-kinematics are on one hand derived from the comparable front axles and on the other hand from the recommendations in [5]. In Fig. 7 the objectives for both the toe angle and camber angle change as well as for the longitudinal and lateral displacement of the wheel center point (WCP) are listed in the order of the respective load transmission.

| | Caster Angle [°/kN] | Camber Angle [°/kN] | Longitudinal WCP- Offset [mm/kN] | Lateral WCP- Offset [mm/kN] |
|------------|------------------------|------------------------|-------------------------------------|--------------------------------|
| Lon. Force | 0 | 0 | 3,0 - 4,0 | 0,2 - 0,3 |
| Lat. Force | 0 | 0 | 0,1 - 0,2 | 0,1 - 0,2 |

Fig. 7: Target Values for the Elasto-Kinematic Behavior of the Front Suspension

The values from the required longitudinal and lateral stiffness should not cause any significant change in the toe angle and camber angle.

3.2 Problem-Solving Process

To design the front suspension while meeting the specified requirements the problem-solving process depicted in Fig. 8 is used. In this process, the work packages and their dependencies are shown.

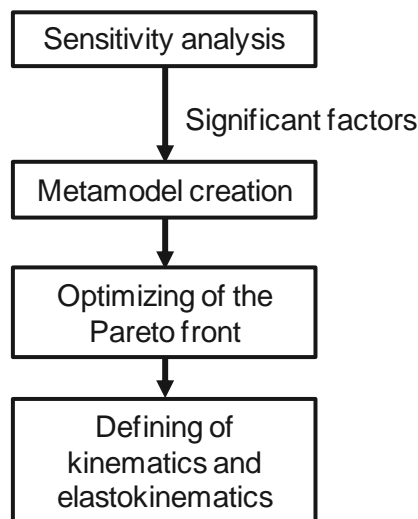


Fig. 8: Problem-Solving Process Diagram

Initially, a sensitivity analysis is performed of the kinematic and elasto-kinematic characteristics of the front suspension. All the parameters are used as factors that have a theoretical influence on the kinematic and elasto-kinematic behavior of the axle. These are the chassis attachment point positions as well as the outer mounting point positions of the control arms, which define the location and orientation of the

steering axis, the angle defining the orientation of the cardan joint axis, and the bushing stiffness. The quality characteristics of the sensitivity analysis are used for the position of the steering axis, the wheel alignment characteristics during parallel wheel travel, steering and under static lateral and longitudinal applied forces, as well as the roll center height during parallel wheel travel and anti-dive compensation. The studies are conducted on a virtual axle measurement rig. The significant factors derived from the sensitivity analysis to influence the behavior of each system can be used to create a meta-model, where a regression model is chosen with a cubic design. In the multi-objective optimization using the genetic algorithm, the meta-model is used to calculate the quality characteristics depending on the selected factors. The goal of the optimization is the approximation of the Pareto-Front to subsequently tune the optimal kinematic and elasto-kinematic characteristics with regards to the construction space limitations. By the determination of the kinematic and elasto-kinematic properties, 16 quality characteristics have to be optimized by means of a genetic algorithm. A simultaneous multi-objective optimization of all 16 criteria as a function of all the selected factors is not effective and no feasible optimization results are achieved.

4 Challenges during the Design Approach

The challenges and solutions by the progressive determination of the kinematics and elasto-kinematics, like those depicted in Fig. 8, are described in the following section.

4.1 Steering Axle Position

With this result of the first optimization run for determining the position of the steering axis in the given space, the maximum potential camber angle of 10° is utilized throughout the complete steering range. Through this, a very small scrub radius of 11 mm is achieved. The associated spread angle increase, which causes a positive camber angle change when steering, is compensated for by a negative caster angle, which causes a negative camber angle change for a positive steering angle of the left wheel. Thus, the 10° camber angle maximum is not exceeded at the critical wheel steering angle of 90° . From the kinematic viewpoint, this configuration is optimal. A problem occurs as a combination of a negative caster angle and a positive caster trail leads to a highly negative caster offset value, see Fig. 6. As a result, the wheel contacts the body structure at a steering angle of 90° ; so this configuration cannot be used. Pictured in Fig. 9 is the position of the steering axis and the corresponding wheel position at 0° und 90° wheel steering angles.

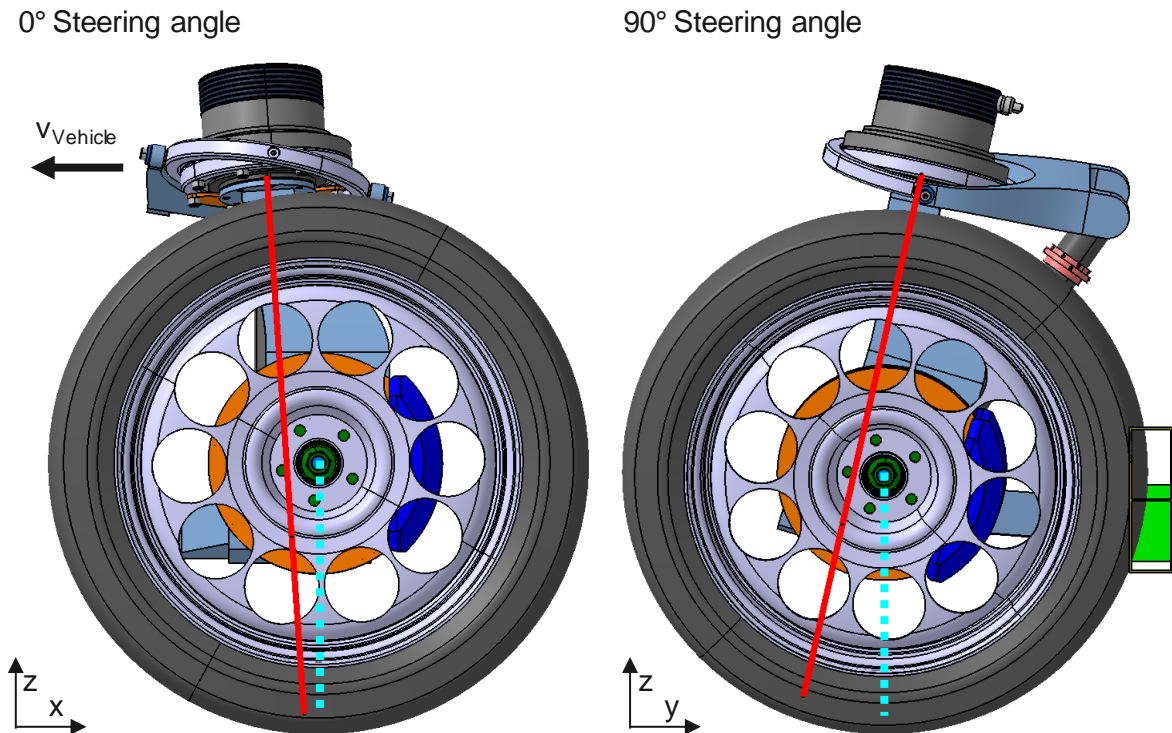


Fig. 9: Steering Axis Position at 0° Wheel Steering Angle (Left) and Wheel Position at 90° Wheel Steering Angle (Right) for the Optimal Kinematic Configuration

In the left and right illustrations, the steering axis is shown solid red and the vertical wheel axis is shown dashed turquoise. In the illustration on the right, in addition to the suspension, a structural part of the body can be seen. It is obvious that the contact of the wheel with the longitudinal member of the body structure is caused by the negative caster offset.

To ensure that the wheel does not move too far from a horizontal steering angle of 90° towards the center plane of the vehicle, the steering axis is positioned in a way that a positive caster offset results. Since the caster trail must have at least 15 mm, a positive caster angle results. The caster trail takes the minimum permitted value, otherwise a positive caster offset increases the caster angle and thus the camber angle at the maximum steering angle of 90° is greater than 10°. In Fig. 10 the wheel position is at 0° and 90° wheel steering angle for the specified steering axis.

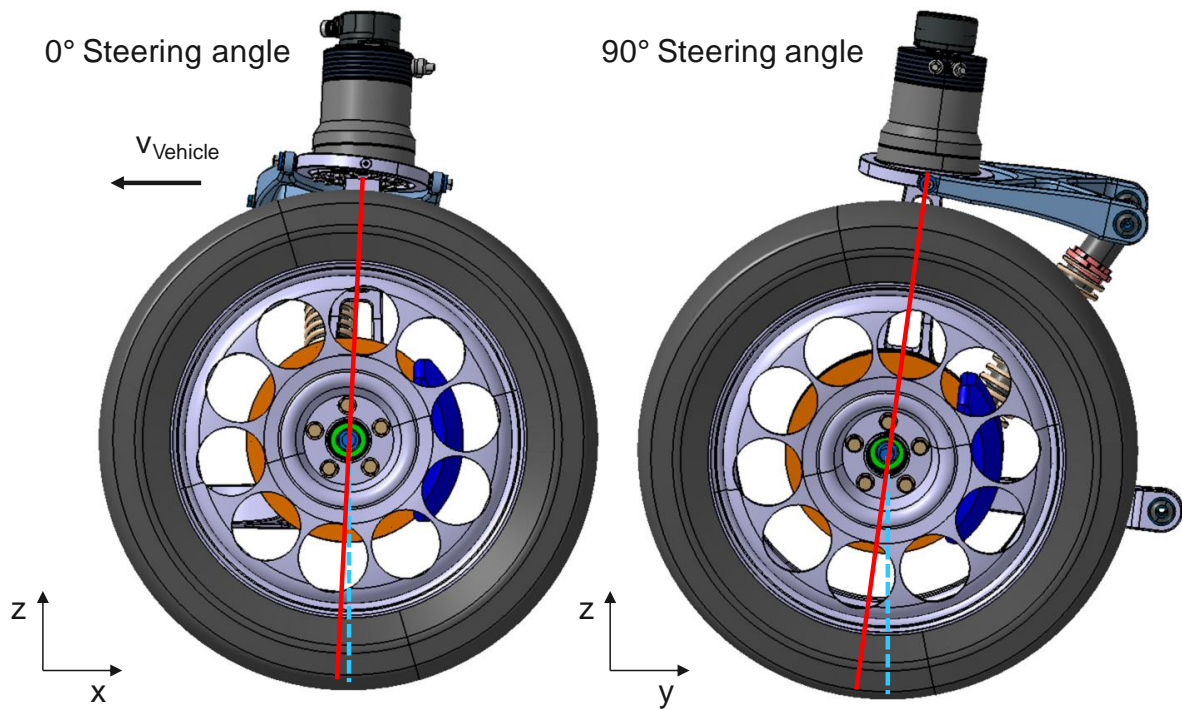


Fig. 10: Position of the Steering Axis at 0° Wheel Steering Angle (Left) and Position of the Wheel at 90° Wheel Steering Angle (Right) Considering the Construction Space Restrictions

It can be seen that because of the positive caster offset, there is no contact between the wheel and the longitudinal member.

In Fig. 11 the resulting camber angle trail is shown as a function of the wheel steering angle. It can be seen that the positive camber change due to the spread angle wheel steering angle is increased by the positive caster angle at 90° and compensated at -60°. To meet the requirement of a maximum camber angle of 10°, a static camber angle of -1° is chosen.

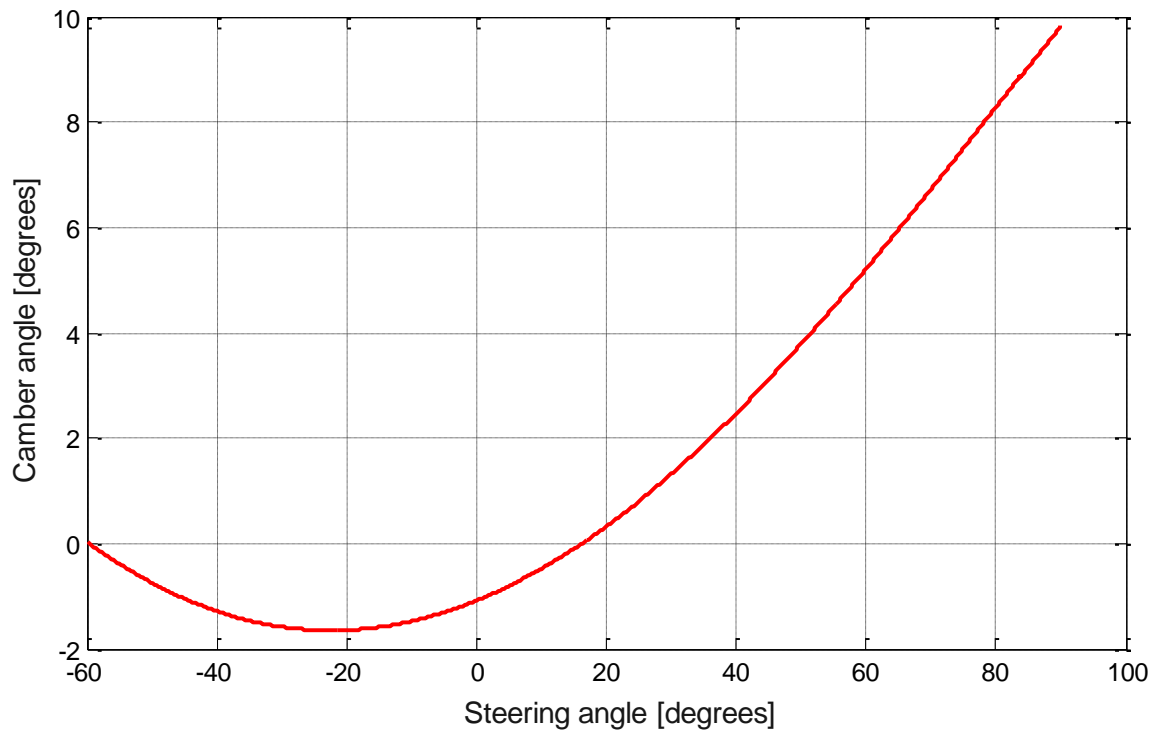


Fig. 11: Camber Angle Course of the Left Front Wheel while Steering

The actually obtained characteristic values of the steering axis are listed in Fig. 12. Additionally, the target values are specified.

| | Scrub Radius [mm] | Caster Trail [mm] | Caster Offset [mm] | Caster Angle [°] | Spread Angle [°] |
|-------|-------------------|-------------------|--------------------|------------------|------------------|
| Tgt. | 0 - 45 | 15 - 45 | - | - | - |
| Actl. | 40,1 | 15,2 | 1,36 | 2,8 | 7,8 |

Fig. 12: Optimized Quality Characteristics of the Steering Axis

4.2 Chassis Attachment Points and Orientation of the Cardan Joint

In Fig. 13 both axes of rotation of the control arm are shown in red and the axis of rotation of the outer cardan ring are shown in green. The axis of rotation of the inner cardan ring is oriented according to the position of the outer cardan ring and the steering axis.

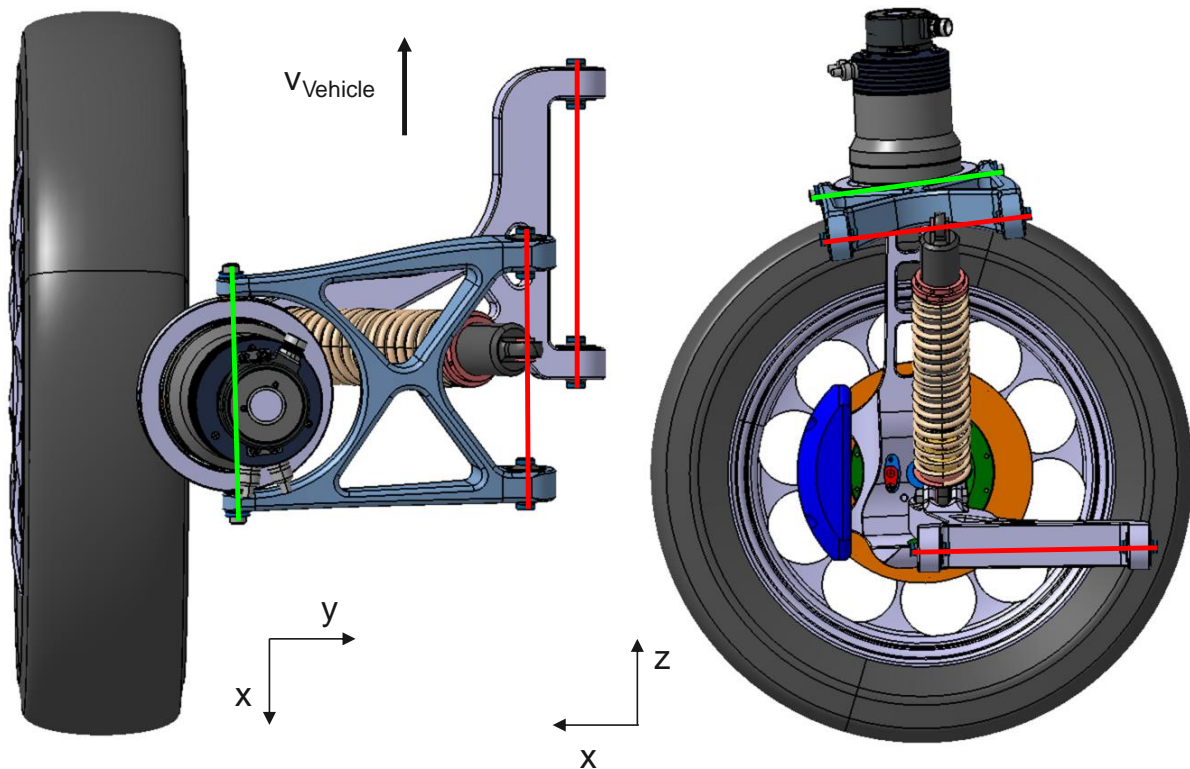


Fig. 13: Position of the Control Arm's Axis of Rotation and the Steering Axle of the outer Cardan Ring

As can be seen in the left side of Fig. 13 the sweep angle of both control arms is zero. As seen in the right side, the axis of rotation of the upper control arm and the steering axis of the outer cardan ring is almost in the same plane. The cardan joint angle β between the steering axle of the outer cardan ring and the global x-y-plane amounts to $\beta = 7.9^\circ$ and the angle between the upper control arm axis of rotation and the x-y-plane amounts to 7.2° . The axis of rotation of the outer cardan ring is slightly rotated outward about the cardan joint angle $\alpha = 1.6^\circ$ corresponding with the global z-x-plane. In particular, the toe angle change during compression is significantly influenced by the position of the cardan joint axis in relation to the steering axis of the upper control arm and through the position of the steering axis.

The unconventional form of the lower control arm is depicted in the left side of Fig. 13. With conventional concepts, the front attachment point of the lower control arm is at the same height as the wheel center point and the rear attachment point is positioned towards the rear of the vehicle. To achieve the 90° wheel steering angle and due to the limited design space an inverted version of the conventional form must be utilized.

Fig. 14 shows the toe angle resultant of the configuration from above, as a function of the wheel travel. It should be noted that the toe angle values are given in angular minutes. The maximum difference of the toe angle as a function of the wheel travel amounts to less than one angular minute. The configuration is adequate to meet the demand of the lowest possible toe angle change during wheel travel.

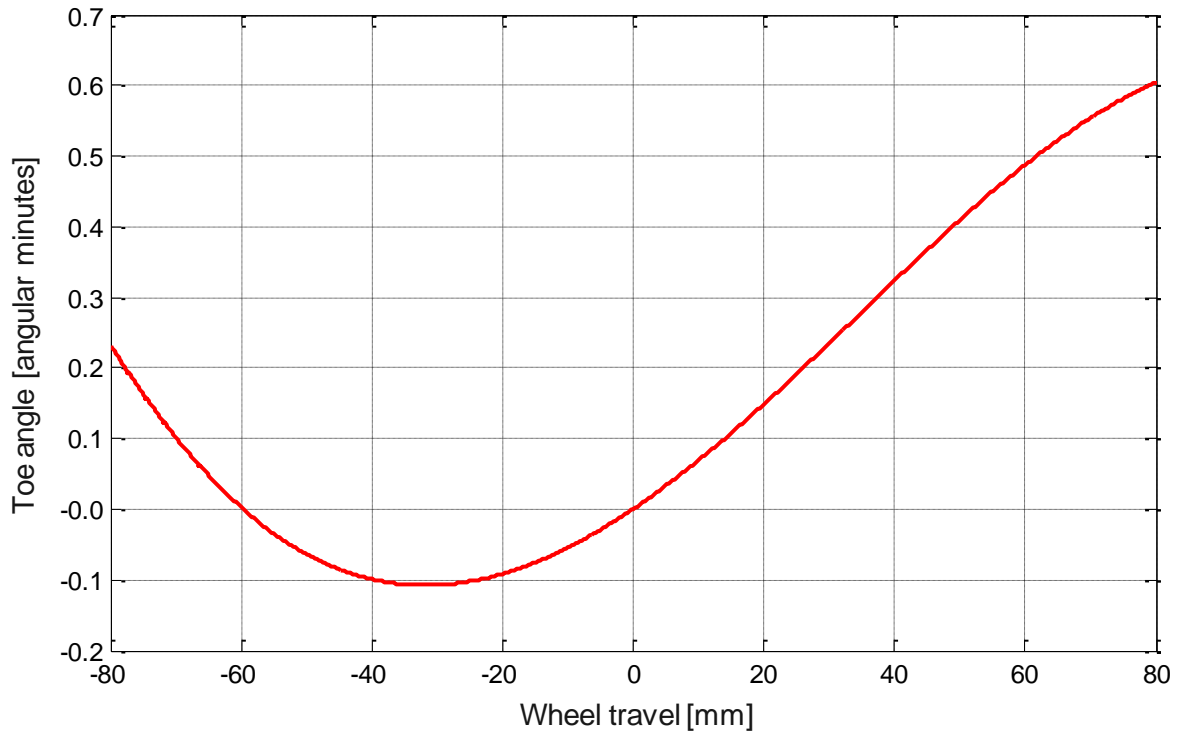


Fig. 14: Toe Angle during Parallel Wheel Travel

The camber angle as a function of the wheel travel is shown in Fig. 15.

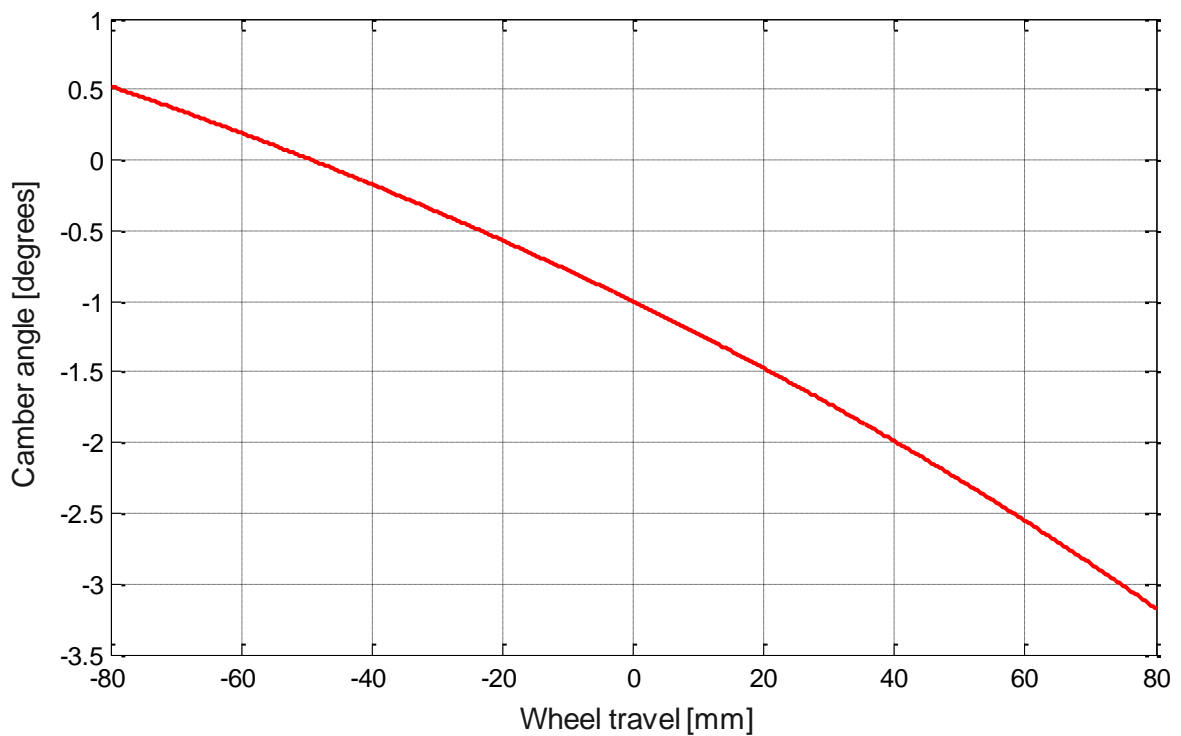


Fig. 15: Camber Angle during Parallel Wheel Travel

The progressive increase of the negative wheel camber under compression is achieved. The roll center height functions of the front and rear axle are depicted in Fig. 16.

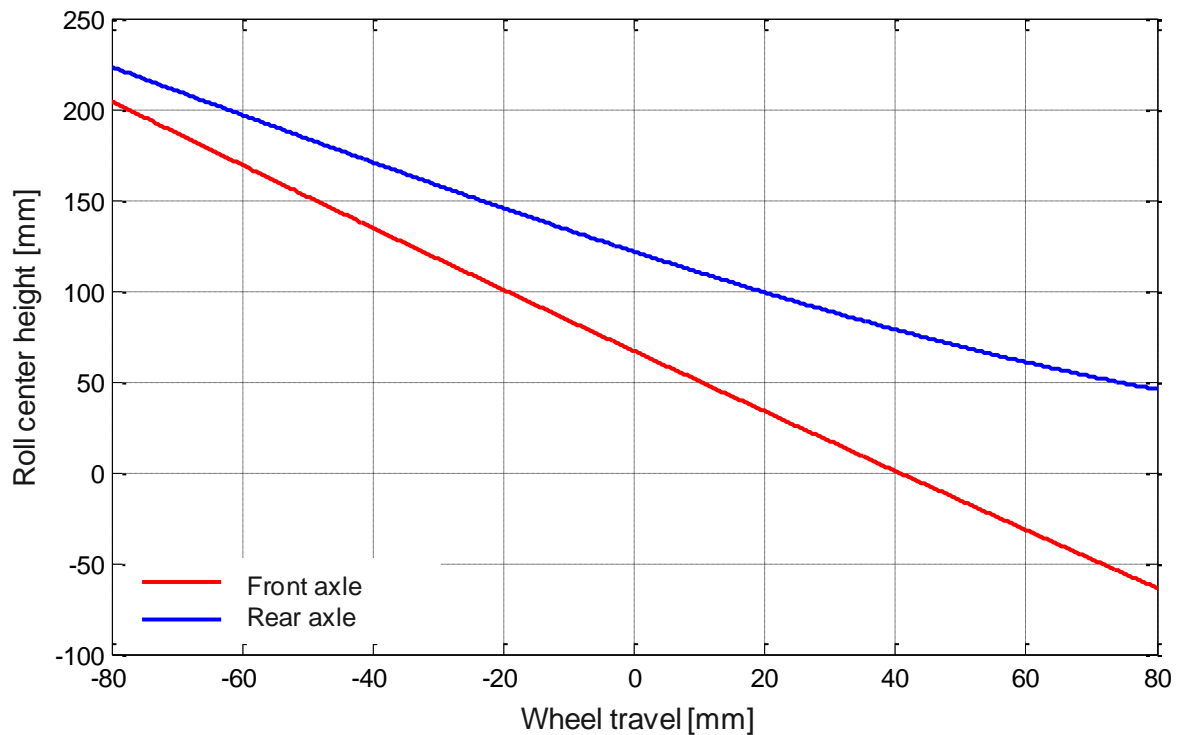


Fig. 16: Roll Center Height at the Front and Rear Axle during Parallel Wheel Travel

The same roll center height change as on the rear axle can be cannot be fully realized because of the shorter upper control arm. Extending the upper control arm is not possible because of the limited available space.

4.3 Bushing Stiffness

In the last step, the bushing stiffness is defined to optimize the elasto-kinematics. Here the toe angle and camber changes, as well as the longitudinal and lateral offset of the wheel center point (WCP) as a result of the applied longitudinal and lateral forces are optimized according to the relevant set requirements. In Fig. 17 the achieved elasto-kinematic characteristics are listed by the longitudinal force application. For comparison the target values are listed as well.

| Longitudinal Force | | | | |
|--------------------|------------------|---------------------|---------------------------------|----------------------------|
| | Toe Angle [°/kN] | Camber Angle [°/kN] | Longitudinal WCP-Offset [mm/kN] | Lateral WCP-Offset [mm/kN] |
| Tgt. | 0,00 | 0,00 | 3,0 - 4,0 | 0,2 - 0,3 |
| Actl. | 0,02 | 0,05 | 3,7 | 0,3 |

Fig. 17: Elasto-Kinematic Characteristics by Longitudinal Force Application

While braking, the wheel toes in by about one angular minute per kilo-newton and experiences a slightly positive change of camber. The required longitudinal elasticity, which is due to the comfort requirements, is achieved. The resulting elasto-kinematic characteristics under application of a lateral force are listed in Fig. 18

| Lateral Force | | | | |
|---------------|---------------------|------------------------|-------------------------------------|--------------------------------|
| | Toe Angle [°/kN] | Camber Angle [°/kN] | Longitudinal WCP- Offset [mm/kN] | Lateral WCP- Offset [mm/kN] |
| Tgt. | 0,00 | 0,00 | 0,1 - 0,2 | 0,1 - 0,2 |
| Actl. | 0,01 | 0,04 | 0,3 | 0,2 |

Fig. 18: Elasto-Kinematic Characteristics by Lateral Force Application

Based on the required elasticity for longitudinal forces, the longitudinal displacement of the wheel center compared to the lateral forces is slightly higher than required but still remains within reasonable limits.

Due to the inverted position of the lower control arm compared to a conventional concept, the rear bushing of the lower control arm has a higher radial stiffness and the front bushing is designed to be softer in radial direction. Thus, for this concept the layout for the handling and comfort bushing are reversed. Both bushings of the upper control arm have the same high stiffness properties as the steering torque is supported by them.

5 Summary

The Institute for Automotive Engineering at RWTH Aachen University (ika), is currently developing, constructing, and implementing the research vehicle SpeedE as an open research and innovation platform for research and industry. The research focus of the SpeedE concept, amongst other things, is the innovative front suspension. Not only is the front axle's steer-by-wire system able to steer each wheel individually, but it is also able to achieve steering angles of up to 90°. These requirements lead to an unconventional setup of the axle replacing the tie rod and the rack and pinion steering gear of a double wishbone suspension by two steering actuators consisting of an electric motor and a harmonic drive reduction gear located at the outer kinematic hardpoint of the upper control arm and mounted to the wishbone through a cardan joint.

This paper describes the development approach to design the kinematic and elasto-kinematic properties of this innovative axle concept by means of genetic algorithm based optimization. Requirements, challenges, and solutions are displayed. A special focus is laid on the effect of the cardan joint on the wheel alignment characteristics.

The optimization is performed in three stages, as a simultaneous optimization of all criteria does not lead to satisfactory results. In the first step, the position of the steering axis is determined. To solve the conflict between the needed space due to the large wheel steering angles and the need to comply with maximum allowable wheel camber, a static camber angle of -1° is ultimately chosen in conjunction with a positive caster trail and a positive caster angle. Subsequently, the chassis attachment points and the orientation of the cardan joint are determined. For this purpose, the orientation of the cardan joint is primarily used to define the toe angle course during wheel travel. Thereby, the requirement is met that the during wheel travel almost no bump toe in occurs. In the third step the determination of the bushing stiffness takes place, such that a sufficient longitudinal elasticity with high transverse rigidity and low impact on the wheel position under the influence of force is achieved.

6 References

- [1] FASSBENDER, S.; ECKSTEIN, L.; HÖREN, B.; STEIN, J.; HESSE, L.; URBAN, P.
Prospects of Holistic Purpose Design by the Example of the Electric Vehicle Concept "SpeedE",
21. Aachener Kolloquium Fahrzeug- und Motorentechnik, Aachen, 2012, pp. 1469-1482.
- [2] N.N.
Nissan Pioneers First-Ever Independent Control Steering Technology,
N.M. Company (Ed.), <http://www.nissan-global.com/EN/DOCUMENT/PDF/TECHNOLOGY/2012/121017-03-e.pdf>, 2012.
- [3] GILLEN, C.; HESSE, L.; MIHAILESCU, A.; ECKSTEIN, L.
Safety strategy for the steer-by-wire system of the research vehicle "SpeedE",
ATZlive (Ed.), Chassis.tech plus 2012, München, 2012, pp. 531-549.
- [4] KLEIN, M.; MIHAILESCU, A.; GILLEN, C.; HESSE, L.; ECKSTEIN, L.
Potentials and Challenges for the Application of Active Sidesticks – Case Study "SpeedE",
21. Aachener Kolloquium Fahrzeug- und Motorentechnik, Aachen, 2012, pp. 663-674.
- [5] HEISSING, B..
Fahrwerkhandbuch
Grundlagen, Fahrdynamik, Komponenten, Systeme, Mechatronik, Perspektiven
Springer Vieweg, Wiesbaden, 2008

